

Vaults in snow constructions

Esko Järvenpää¹, Antti H. Niemi and Matti-Esko Järvenpää

Summary The article discusses the principles of arch design as they apply to snow vaults and presents different types such as parabolic, catenary, circular and constant stress. The parabolic momentless arch requires a constant vertical load throughout the span, resulting in a decreasing snow thickness from the crown to the base. In contrast, the catenary arch is formed by an inverted hanging chain, maintaining a uniform snow thickness throughout the structure, governed by a hyperbolic cosine function. The shape of the constant stress standalone arch is determined by the unit weight and the compressive stress, described by a logarithmic cosine function. In comparing snow arches, the article asserts the superiority of the constant stress form over the catenary and parabolic forms, highlighting its ability to span greater distances. Despite its advantages, the constant stress form has not yet found application in the construction of snow vaults. In addition, snow vaults are subject to significant deformation and require regular checks and recalculations throughout their life to ensure structural integrity.

Key words: snow constructions, arch, vault, constant stress vault

Received: 20 May 2024. *Accepted:* 20 November 2024. *Published online:* 18 December 2024.

Introduction

In the design of snow structures, achieving a compression stress structure is both a realistic and attainable goal. In Finland, the RIL 218-2001 guideline provides a pragmatic approach to achieving this objective. The guideline requires the performance of static calculations for snow structures, with simplified instructions provided for those that have not undergone separate structural calculations [1]. The Lapland University of Applied Sciences has released a practical guide for the design of snow and ice structures based on field tests [2]. The guide is intended for designers and authorities responsible for implementing snow structures. This article provides further information that may indicate additions to the published documents.

To ensure a cross-section without tensile stress in the arch, the thrust line must be located in the middle third of the arch rib cross-section. The thrust line theory is a historically familiar concept as a design principle for stone and concrete vaults. It has

¹ Corresponding author: eojarvenpaa@gmail.com

been assumed that compressive strength is not critical to the load-bearing capacity of the vault in stone structures [3]. However, this assumption does not hold true for snow structures.

When designing and constructing snow and ice structures, it is important to ensure that the thrust line runs along the axis of gravity of the structure. The moment-free form can only be achieved for permanent loads, as all other variable loads impose bending stresses.

In snow structures, the primary load is the weight of the snow. Therefore, the emphasis is on designing the shape. The magnitude of the permanent load in snow structures can be monitored, and if necessary, corrected to match the optimal shape.

Research has found that the parabolic shape is the most efficient in terms of material flow when supporting an evenly distributed vertical load between two support points [4]. The arch is then compressed centrally. The compression stress is lowest for the parabolic moment-free standalone arch at its base when the span length to height ratio l/h is 4.

Robert Hooke first published the principle of the catenary arch in 1675 [5]. He recognized that the arch was not a parabola but was unable to determine its mathematical solution [6]. The equation for the shape of the arch was published in 1691, after the development of differential and integral calculus [7], [8], [9]. This study shows that for a standalone catenary arch, the lowest compressive stress at the base is obtained when the rise ratio is 2.96.

The arch can be designed to maintain a constant compressive stress throughout the structure. An analytical solution for this type of arch has been derived [10], [11]. The design of arched structures has only been studied in recent years [12].

The constant stress shape allows for much longer spans than the parabola or the catenary [13]. The low compressive stress of the constant stress arch is a significant advantage for snow vault structures.

The circular shape is suitable for compressive loads, but not for vertical loads [14]. If you want to construct an independent circular vault with no moment, you will need to increase the thickness of the vault as you increase its height. Only with flat arch shapes is the circular shape of the vault a viable option. It is important to note that the circular shape is not included in the comparison calculations between the vaults in this study.

The shape of the momentless arch does not precisely follow the above shape along the centroidal axis. The arch rib thickness and cross-sectional curvature affect the transfer of the centre of gravity above the central axis. This is because the upper soffit of the arch is longer than the lower soffit [15]. This article will not discuss this topic further.

The inner soffit of the vault does not have the same shape as the shape according to the axis of gravity, which affects the shape of the vault form due to the thickness of snow structures in cross-section.

Snow and ice are frequently used as temporary building materials in cold regions, particularly in popular tourist destinations. The traditional form of snow structure used in Greenland and Alaska is the igloo [16]. The annual snow sculpture festival in Harbin, China is likely the largest tourist event in the world. In Finland, snow structures are built annually in Kemi and Kittilä.

Artificial snow is typically used to construct snow structures. The material properties of snow can be described by various factors, including density, compressive strength, tensile strength, creep, viscosity, and coefficient of elasticity.



Figure 1. Snow castle in Kemi, Finland (2019). Photo Esko Järvenpää.

The eccentricity of the compressive force, resulting from the relatively rapid compression and settlement of the snow structure, affects the bending moments and shear forces. These, in conjunction with the changing environmental conditions, can lead to the collapse of the snow vault. Should the shape of the snow vault undergo alteration, it is imperative to undertake a calculation of the resulting stresses and evaluate the condition of the structure in accordance with the new calculations. The settlement should be limited to the previously specified limit, based on site-specific calculations. Correction of the settled snow structure should not be made by increasing the thickness of the snow.

Vault forms

Parabolic vault

The equation for the parabolic vault in the coordinate system shown in Figure 2 is given by

$$y = -\frac{4h}{l^2}x^2 + h, \quad -\frac{l}{2} < x < \frac{l}{2}. \quad (1)$$

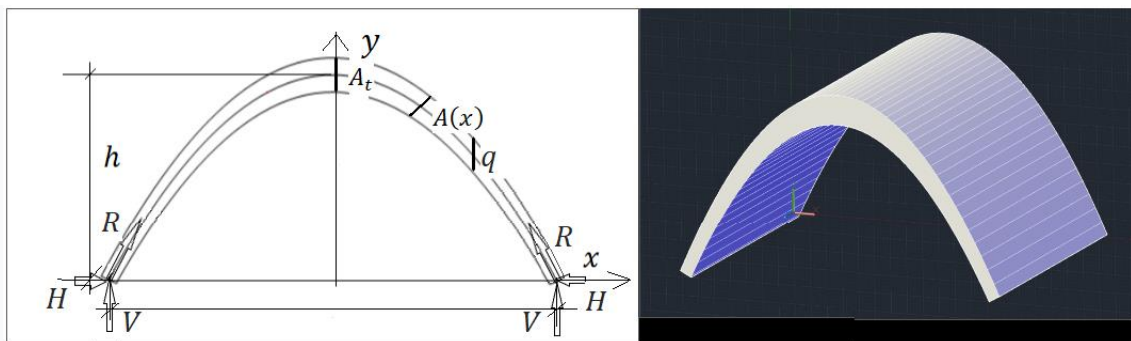


Figure 2. Parabolic vault, and an example vault with the rise ratio $l/h = 2$.

The horizontal force H acting on the vault, corresponding to the vertical load q per unit length of the x -axis, is then given by

$$H = \frac{ql^2}{8h} \quad (2)$$

and the normal force $R(x)$ of the vault at point x is

$$R(x) \equiv H\sqrt{1 + y'(x)^2} = \frac{ql^2}{8h} \sqrt{1 + \frac{64h^2x^2}{l^4}}. \quad (3)$$

Consequently, the normal force at the base of the vault is

$$R_b \equiv R\left(\frac{l}{2}\right) = \frac{ql^2}{8h} \sqrt{1 + \frac{16h^2}{l^2}}. \quad (4)$$

If we denote the area of the cross-section at the vertex by A_t , then the area of the cross-section $A(x)$ is

$$A(x) = \frac{A_t}{\sqrt{1 + y'(x)^2}} = \frac{A_t}{\sqrt{1 + \frac{64h^2x^2}{l^4}}}. \quad (5)$$

The compressive stress σ_b at the base is obtained with the help of Equations (4) and (5) and the relation $q = \gamma A_t$, where γ is the unit weight of the snow material. The result is

$$\sigma_b \equiv \sigma(l/2) = \frac{R(l/2)}{A(l/2)} = \gamma \left(\frac{l^2}{8h} + 2h \right). \quad (6)$$

Equation (6) can be written as

$$\sigma_b = k_p \gamma l, \quad (7)$$

where k_p is called stress coefficient and is obtained from

$$k_p = \frac{l}{8h} + \frac{2h}{l}. \quad (8)$$

The coefficient k_p in terms of rise ratio l/h is shown graphically in Figure 3. Minimising the coefficient k_p as a function of height h gives

$$\frac{dk_p}{dh} \equiv -\frac{l}{8h^2} + \frac{2}{l} = 0 \rightarrow h = \frac{l}{4} \rightarrow k_p = 1. \quad (9)$$

Thus, the normal stress $\sigma_b = k_p \gamma l$ gets its minimum

$$\sigma_{b\min} = \gamma l, \quad (10)$$

when the rise ratio $l/h = 4$ (compare Figure 3). The maximum span length l_{pmax} of a momentless standalone parabolic vault, when the compressive stress is used as criterion, is obtained by setting $\sigma_b = \sigma_{adm}$, where σ_{adm} is the admissible stress of snow and using Equation (7). The result is

$$l_{pmax} = \frac{\sigma_{adm}}{k_p \gamma}. \quad (11)$$

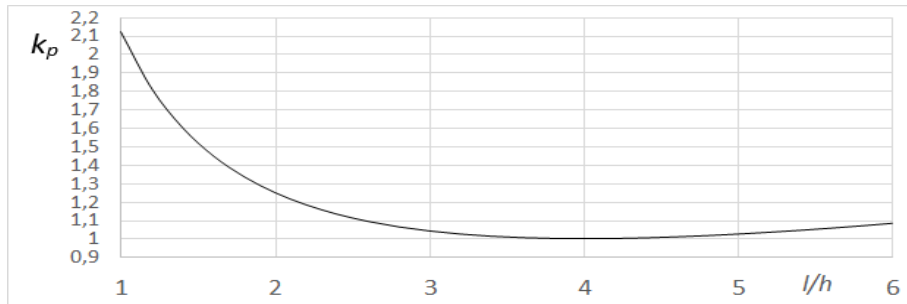


Figure 3. Stress coefficient k_p of parabolic momentless standalone vault at the base.

Catenary vault

The equation for the catenary in the coordinate system shown in Figure 4 is

$$y(x) = a \left(1 - \cosh \frac{x}{a} \right) + h, \quad -\frac{l}{2} < x < \frac{l}{2}, \quad (12)$$

where $a = H/w$. Here, H represents again the horizontal force and w represents the weight of the vault per unit length. The normal force $R(x)$ at point x gets the form

$$R(x) \equiv H \sqrt{1 + y'(x)^2} = H \sqrt{1 + \left(\sinh \frac{x}{a} \right)^2} = H \cosh \frac{x}{a}. \quad (13)$$

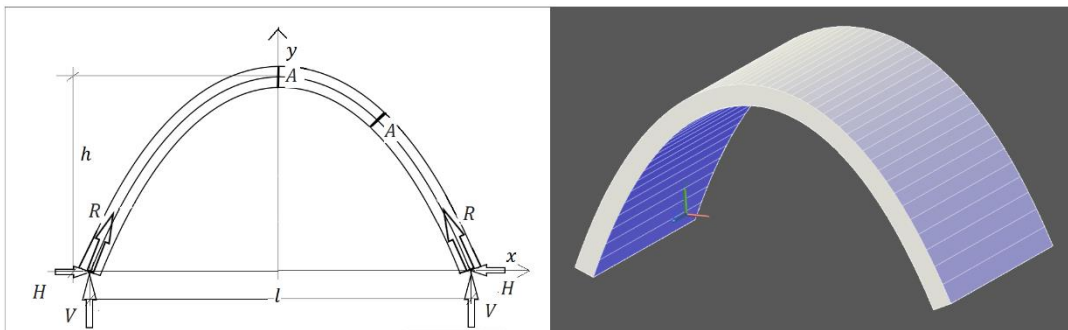


Figure 4. Catenary vault, and example vault with rise ratio $l/h = 2.0$.

The expression for the normal force R_b at the base is then

$$R_b \equiv R\left(\frac{l}{2}\right) = H \cosh \frac{l}{2a} = aw \cosh \frac{l}{2a} \quad (14)$$

and the normal stress σ_b at the base further

$$\sigma_b \equiv \frac{R_b}{A} = \frac{aw}{A} \cosh \frac{l}{2a} = a\gamma \cosh \frac{l}{2a} \quad (15)$$

or

$$\sigma_b = k_c \gamma l, \quad (16)$$

where

$$k_c = \frac{a}{l} \cosh \frac{l}{2a} \quad (17)$$

is the corresponding stress coefficient.

With $y = 0$ and $x = l/2$ Equation (10) gives

$$h = a \left(\cosh \frac{l}{2a} - 1 \right). \quad (18)$$

This Equation can be written as

$$\frac{a}{l} \left(\cosh \frac{l}{2a} - 1 \right) - \frac{h}{l} = 0. \quad (19)$$

This is a nonlinear equation, which can be used to solve the ratio a/l corresponding to a given ratio l/h . The stress coefficient k_c corresponding to a given rise ratio l/h can be determined by first solving the ratio a/l from Equation (19) and then using Equation (17). The stress coefficient k_c in terms of rise ratio l/h is shown graphically in Figure 5.

Minimizing the stress coefficient k_c with respect to the parameter a gives

$$\frac{dk_c}{da} \equiv \frac{1}{l} \cosh \frac{l}{2a} - \frac{1}{2a} \sinh \frac{l}{2a} = 0 \rightarrow \frac{2a}{l} = \tanh \frac{l}{2a}. \quad (20)$$

Solution of this nonlinear equation is $a = 0.416778l$. The corresponding stress coefficient is obtained using Equation (17):

$$k_c = 0.416778 \cdot \cosh \frac{1}{2 * 0.416778} = 0.754440. \quad (21)$$

Substituting this into Equation (18) gives

$$h = 0.416778l \cdot \left(\cosh \frac{1}{2 \cdot 0.416778} \right) = 0.337662l \quad (22)$$

and the corresponding rise ratio is $l/h = 1/0.337662 = 2.961533$. Thus the normal stress σ_b attains its minimum $\sigma_{cmin} = 0.754a$, when $l/h = 2.96$ (compare Figure 5).

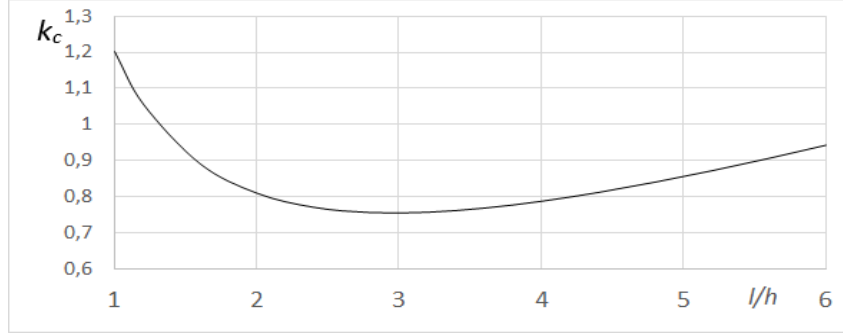


Figure 5. Stress coefficient k_c of standalone catenary vault at the base.

The maximum span length l_{cmax} of a momentless standalone catenary vault, when the compression stress is used as the criterion, is obtained by setting $\sigma_b = \sigma_{adm}$, where σ_{adm} is admissible compressive stress of snow. Using Equation (16) one obtains

$$l_{cmax} = \frac{\sigma_{adm}}{k_c \gamma}. \quad (23)$$

Circular vault

Similarly, as above, the axis of gravity of the circular vault can be expressed as a function of its span length l and height h as follows:

$$y = \left(\frac{1}{8h} \right) \left(4h^2 - l^2 + \sqrt{-64x^2h^2 + 16h^4 + 8h^2l^2 + l^4} \right). \quad (24)$$

Figure 6 demonstrates the rapid increase in thickness of the circular vault towards the base. The stress in the arch decreases from the top to the base [17]. The circular shape for vertical loads as a momentless structure is a viable option for low arches. However, snow arches tend to favour higher arches, which is why the circular vault is not discussed further in this article. Furthermore, Figure 12 illustrates the difference between a standalone circular vault and other vault types discussed in this article.

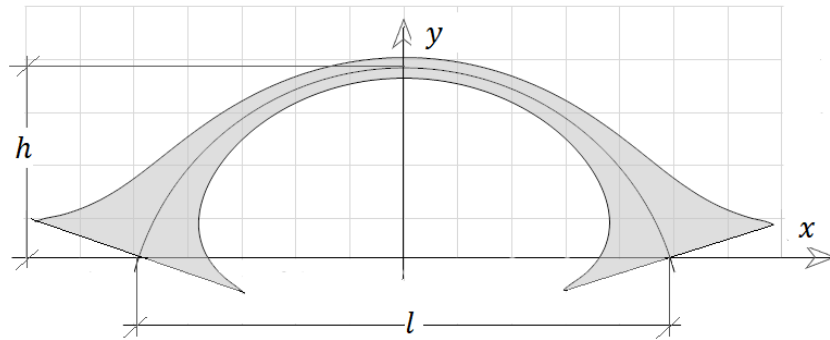


Figure 6. An example of a standalone momentless circular vault.

Constant stress vault

The constant stress vault equation, according to the coordinates in Figure 7, is

$$y(x) = b \ln \left(\cos \frac{x}{b} \right) + h, \quad -\frac{l}{2} < x < \frac{l}{2}. \quad (25)$$

where $b = \sigma/\gamma$. The symbol γ is the unit weight of the material [MN/m³] and σ is the constant stress level in the vault [MPa].

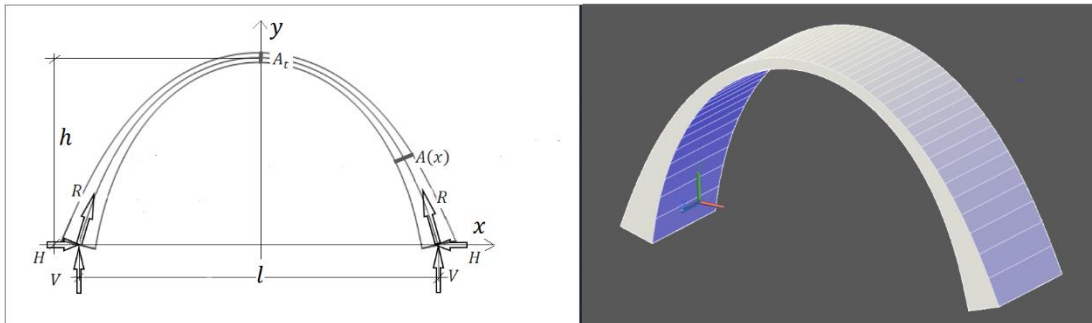


Figure 7. Constant stress vault and an example of a constant stress vault with a rise ratio $l/h = 2$.

The normal force $R(x)$ at point x is

$$R(x) \equiv H \sqrt{1 + y'(x)^2} = H \sqrt{1 + \left(\tan \frac{x}{b} \right)^2} = \frac{H}{\cos \frac{x}{b}}. \quad (26)$$

By denoting the area of the top cross-section as A_t , the horizontal force H is

$$H = A_t \sigma. \quad (27)$$

Based on relation $\sigma = R/A$, the area of the cross-section $A(x)$ has the form

$$A(x) \equiv \frac{R(x)}{\sigma} = \frac{H}{\sigma \cos \frac{x}{b}} = \frac{A_t}{\cos \frac{x}{b}}. \quad (28)$$

With $y = 0$ and $x = l/2$ Equation (25) gives

$$h = -b \ln \left(\cos \frac{l}{2b} \right). \quad (29)$$

The stress $\sigma = \gamma b$ can be written as

$$\sigma = k_{cs} \gamma l, \quad (30)$$

where

$$k_{cs} = b/l \quad (31)$$

is the corresponding stress coefficient. Equation (29) can then be written as

$$\frac{b}{l} \ln \left(\cos \frac{l}{b} \right) + \frac{h}{l} = 0. \quad (32)$$

This is a nonlinear equation, which can be used to solve the ratio b/l corresponding to a given rise ratio l/h . The stress coefficient k_{cs} corresponding to a given rise ratio l/h is obtained first solving the ratio b/l from Equation (32) and then using Equation (31). The stress coefficient k_{cs} in terms of the rise ratio l/h from 1 to 6 is presented graphically in Figure 8.

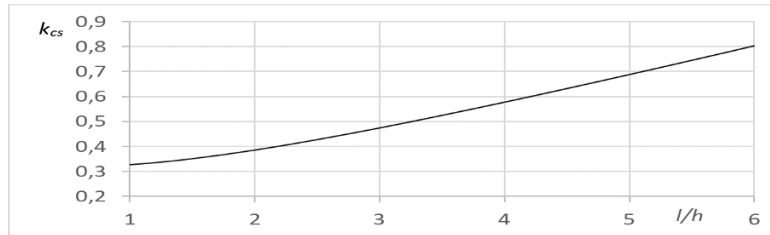


Figure 8. Stress coefficient k_{cs} of constant stress standalone vault.

Comparison of stresses in the vaults

Above, we introduced the stress calculation coefficients k_p , k_c , and k_{cs} . Figure 9 combines the results and shows the stress magnitudes in the momentless vaults in the same figure as a function of the rise ratio.

Figure 9 illustrates that the higher the vaults are, the more they differ from each other, and the benefit of the constant stress vault is remarkable. For instance, at a rise ratio of 2, a catenary has twice the stress level of a constant stress vault. This information may also be useful for weak materials other than low strength snow.

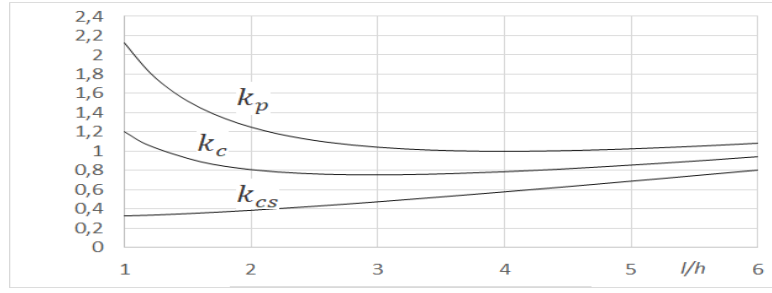


Figure 9. Stress coefficients of parabola, catenary and constants stress vault in standalone vaults.

Extreme span of constant stress vault

The minimum stress coefficient k_{cs} is achieved by decreasing the rise ratio l/h to zero. In this case Equation (32) gives $\ln(\cos l/2b) = -\infty$, $l/b = \pi$. Thus, the minimum stress coefficient of the constant stress vault is $k_{cs} = 1/\pi = 0.3183$.

The maximum span length l_{csmax} of a standalone constant stress vault, when the compression stress is used as criterion, is obtained by setting $\sigma_b = \sigma_{adm}$, where σ_{adm} is the admissible compressive stress of snow. Using Equation (30) one obtains

$$l_{csmax} = \frac{\sigma_{adm}}{k_{cs}\gamma}. \quad (33)$$

The ultimate asymptotical span length corresponds to $l/h = 0$ and $k_{cs} = 1/\pi$ resulting to

$$l_{ult} = \frac{\pi\sigma_{adm}}{\gamma}, \quad (34)$$

see [10]. The height of the arch is limited by its weight at the base. To maintain a constant stress shape, the rise of the vault, which causes the cross-sections to meet at the base, is illustrated in Figure 10. Using Equation (28) with $A(x) = d(x) \cdot 1$ m gives

$$d_b \equiv d\left(\frac{l}{2}\right) = \frac{d_t}{\cos \frac{l}{2b}} = \frac{d_t}{\cos \frac{\gamma l}{2\sigma}} \quad (35)$$

and noting that

$$d_b = l \frac{\sqrt{1 + y'(x)^2}}{y'(x)} = l \frac{\sqrt{1 + \left(\tan \frac{l}{2b}\right)^2}}{\tan \frac{l}{2b}} = \frac{l}{\sin \frac{l}{2b}} = \frac{l}{\sin \frac{\gamma l}{2\sigma}}. \quad (36)$$

The equation for solving the vault span is therefore

$$l - d_t \tan \frac{\gamma l}{2\sigma} = 0. \quad (37)$$

To illustrate, if we substitute $\gamma = 0.006 \text{ MN/m}^3$, $\sigma = 0.200 \text{ MPa}$ and $d_t = 4 \text{ m}$ the solution is $l = 102.110 \text{ m}$. Subsequently, equation (29) gives $h = 108.209 \text{ m}$ and the rise ratio becomes $l/h = 0.944$, (compare Figure 10).

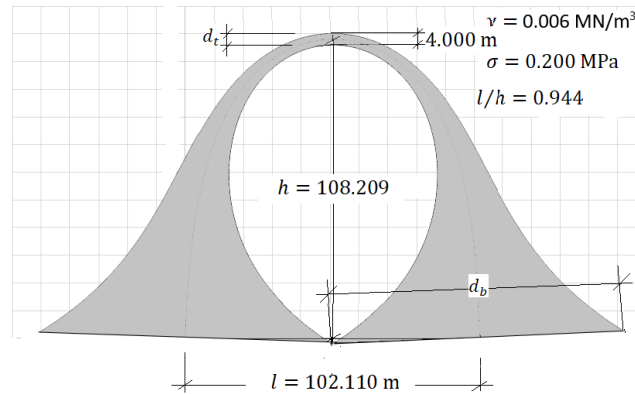


Figure 10. The maximum span length of a snow vault. The unit weight and the stress used are chosen values.

Calculation examples

Shape difference of the vaults

For the following example, the circular, constant stress, catenary and parabolic standalone momentless vault shapes have been calculated using a span of 12 m and a height of 6 m. For the catenary vault, the parameter a has first been solved using Equation (12) from the boundary conditions $y = 0$ and $x = 6$, and consequently the parameter b for the constant stress vault using Equation (25). The unit weight of snow is $\gamma = 0.006 \text{ MN/m}^3$. The difference of the shapes is demonstrated in Figure 11.

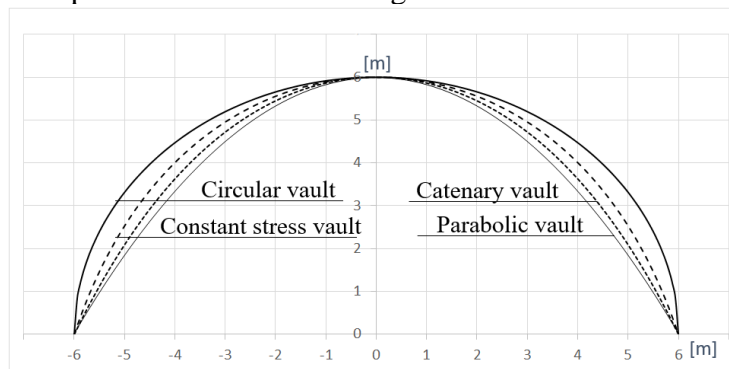


Figure 11. The shapes of circular, constant stress, catenary and parabolic snow vaults for $l/h = 2$.

Comparison of the thickness of snow in the vaults

Each type of arch requires a different vertical load for the independent momentless form. The vertical snow thicknesses of the arches of equal thickness at the apex are shown in

Figure 12 for the rise ratio $l/h = 2$. Furthermore, Figure 13 illustrates the cross-sections of the same vaults.

It is worth noting that the illustrative thicknesses in Figure 12 and the cross-section in Figure 13 do not indicate that the vaults are comparative alternative vaults. This is because their compressive stresses are calculated using the same thickness of 2 m at the apex.

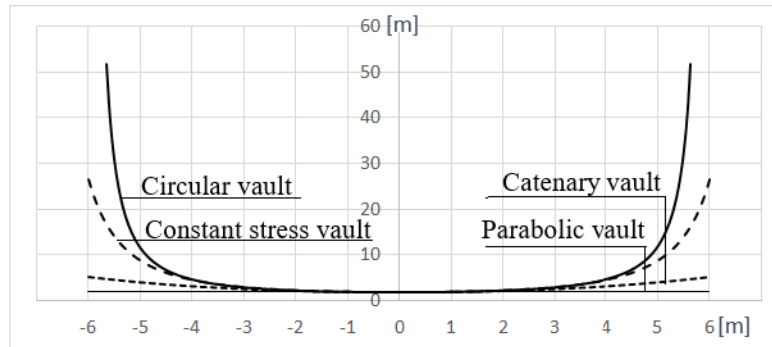


Figure 12. The vertical thickness of the momentless standalone snow vaults when $l/h = 2$.

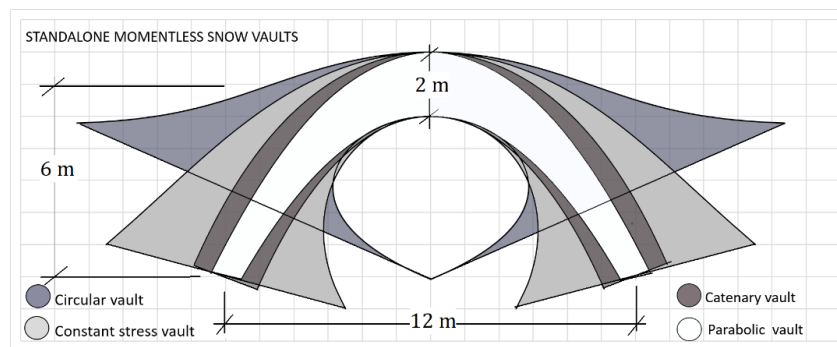


Figure 13. Demonstration of the snow vaults for $l/h = 2$ with equal apex thicknesses.

Rise ratio and shape in constant stress vault

For the following example, four constant stress vaults are calculated using Equations (25) and (28). Figure 14 shows the vaults with rise ratios of $l/h = 1.5, 2.0, 4.0$ and 6.0 when the unit weight of snow is $\gamma = 0.006 \text{ MN/m}^3$. The figure also shows the stresses and the bottom areas in the vaults. The stresses have been determined by first solving the ratio b/l from Equation (32) and then using Equations (31) and (30). The bottom areas have been obtained using Equation (29) with $x = l/2$.

Illustrative comparison of vault shapes and spans

The characteristics of cross-sections of momentless parabolic, catenary and constant stress vaults were presented in the previous section. Comparative calculations and 3D modelling were carried out for each type of arch. The snow vaults had the same structural thickness at the crown and experienced a maximum compressive stress of 0.15 MPa. The rise ratio used was 2.0. Figure 15 shows the shapes and sizes of the calculated vaults on

the same scale. The superiority of the constant stress vault in terms of span length over the corresponding parabolic and catenary vaults is evident.

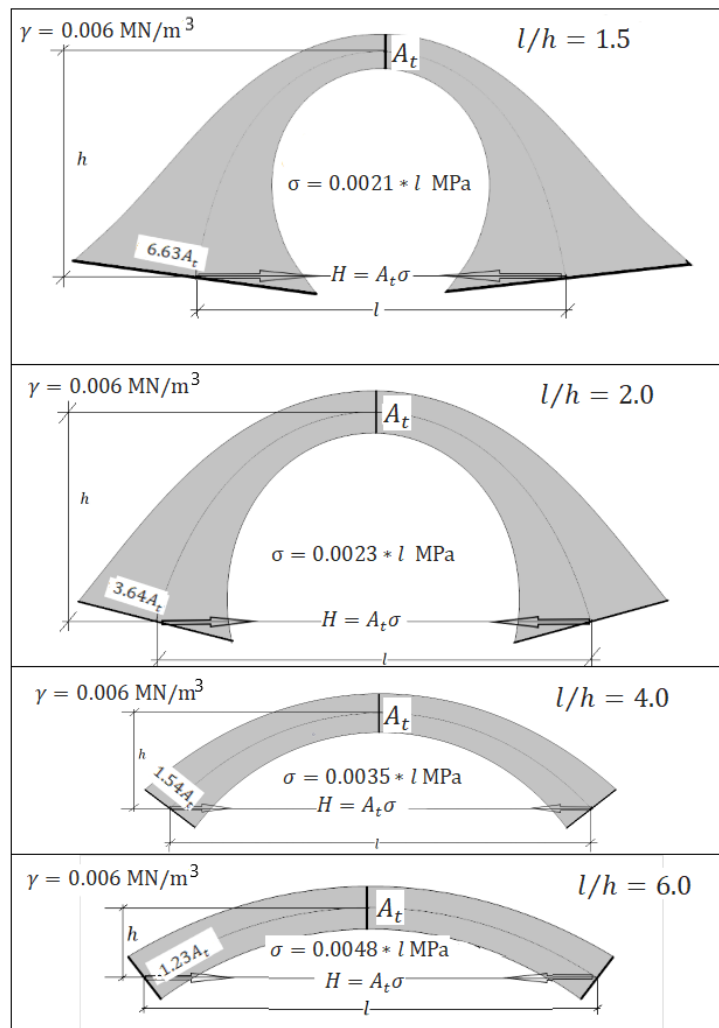


Figure 14. Examples of constant stress snow vaults with rise ratios of 1.5, 2.0, 4.0, and 6.0.

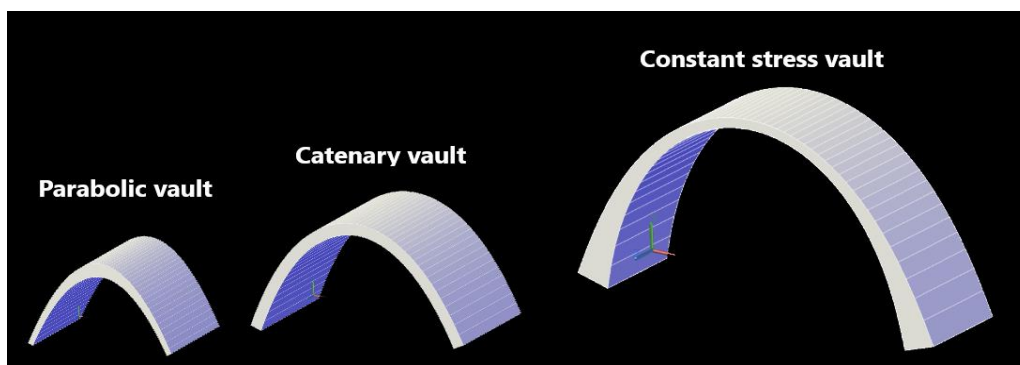


Figure 15. Comparison of snow vaults with a stress level of 0.15 MPa and the rise ratio of 2.0.

Snow volumes based on rise ratio

The volumes of parabolic, catenary, and constant stress arches are calculated using their respective volume coefficients k_{pvol} , k_{cvol} , and k_{csvol} . These coefficients are calculated and displayed graphically in Figure 16.

The volume of a vault of a cross-section area $A(x)$ is obtained from

$$V_{\text{vol}} = \int_{-\frac{l}{2}}^{\frac{l}{2}} A(x) ds(x) = \int_{-\frac{l}{2}}^{\frac{l}{2}} A(x) \sqrt{1 + y'(x)^2} dx. \quad (38)$$

For parabolic vault, we get

$$V_{\text{pvol}} = 2 \int_{-\frac{l}{2}}^{\frac{l}{2}} \frac{A_t}{\sqrt{1 + \frac{64h^2x^2}{l^4}}} \sqrt{1 + \frac{64h^2x^2}{l^4}} dx = A_t l. \quad (39)$$

For catenary vault, we get

$$V_{\text{cvol}} = \int_{-\frac{l}{2}}^{\frac{l}{2}} A \sqrt{1 + \left(\sinh \frac{x}{a}\right)^2} dx = A \int_{-\frac{l}{2}}^{\frac{l}{2}} \cosh \frac{x}{a} dx = \frac{2a}{l} \sinh \frac{l}{2a} A l. \quad (40)$$

For constant stress arch, we get

$$V_{\text{csvol}} = \int_{-\frac{l}{2}}^{\frac{l}{2}} \frac{A_t}{\cos \frac{x}{b}} \sqrt{1 + \left(\tan \frac{x}{b}\right)^2} dx = 2A_t \int_{-\frac{l}{2}}^{\frac{l}{2}} \frac{1}{\left(\cos \frac{x}{b}\right)^2} dx = \frac{2a}{l} \tan \frac{l}{2b} A_t l. \quad (41)$$

These results can be summarised as

$$V_{\text{pvol}} = k_{\text{pvol}} A_t l, \quad V_{\text{cvol}} = k_{\text{cvol}} A l, \quad V_{\text{csvol}} = k_{\text{csvol}} A_t l, \quad (42)$$

where the volume coefficients are

$$k_{\text{pvol}} = 1, \quad k_{\text{cvol}} = \frac{2a}{l} \sinh \frac{l}{2a}, \quad k_{\text{csvol}} = \frac{2a}{l} \tan \frac{l}{2b}. \quad (43)$$

the ratios a/l and b/l corresponding to given rise ratio l/h are obtained by solving the Equations (19) and (32).

Figure 16 illustrates the volumes of snow in different vault types when the cross-sectional areas at the crown are equal. Figure 16 is divided into two parts. This is due to the fact that the volume of the constant stress vault changes significantly as the height of the vault increases. As the height decreases, the volumes of the catenary and constant stress vaults approach the volume of the parabola.

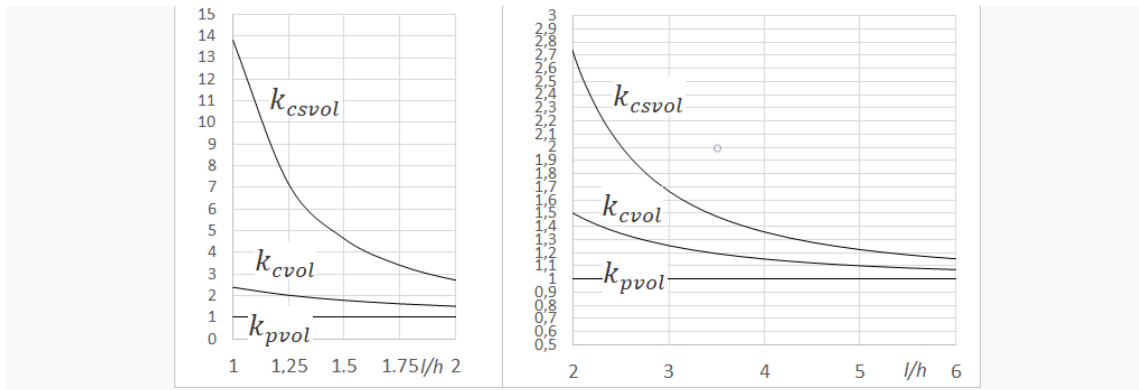


Figure 16. Vault volume coefficients k_{pvool} , k_{cvool} , and k_{csvol} , according to rise ratios.

Comparison example of stresses and snow volumes

Table 1 shows the calculated stresses and volumes of parabolic, catenary, and constant stress vaults, highlighting the differences between the types. The calculations were based on the formulas previously introduced.

The vaults have a snow thickness of one metre at the crown, a span of 15 m and a height of 7.5 m. The stresses and volumes of snow have been calculated for a vault strip of one metre. The unit weight used was 0.005 MN/m^3

Table 1. Stresses and snow volumes in the example vaults.

Vault type	Span [m]	Height [m]	Stress [MPa]	Volume [m ³]
Parabola	15.0	7.5	0.08	15.0
Catenary	15.0	7.5	0.06	22.5
Constant stress	15.0	7.5	0.03	40.5

The volume of the constant stress vault, with the same thickness at the apex as the parabola and the catenary, is significantly greater than the volumes of the parabola and the catenary. In practice, the constant stress vault does not necessarily require the same thickness due to the thickening of the cross-section towards the base.

Comparison of extreme span lengths for parabola, catenary and constant stress vaults

Figure 17 shows the maximum span lengths of the freestanding parabolic, catenary and constant stress vault according to the maximum compressive stress. For the parabolic and catenary arches, the critical point is at the base of the arch, while for the constant stress vault, the stress is constant along the entire length of the arch. The assumed compressive stress limit of the snow is 0.2 MPa. The unit weight of snow used is 0.006 MN/m^3 . The stability of the structure is not specified. The thickness of the arch at the crown can be chosen arbitrarily as it has no effect on the magnitude of the stresses. The calculation

result describes the situation at time $t = 0$. In this case, it is assumed that the compression of the snow is eliminated by increasing the horizontal force of the arch to match the horizontal force of the uncompressed arch.

The maximum span length of a parabolic vault is terms of the rise ratio can be determined using Equations (8) and (11). The maximum span lengths of catenary and constant stress vaults can be determined by first solving Equations (19) and (32) for the ratios a/l and b/l , respectively, and then using Equations (23) and (33).

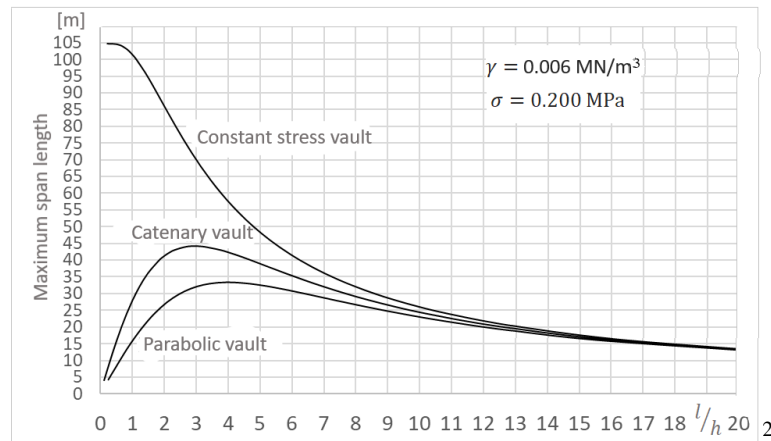


Figure 17. The maximum span lengths of the parabolic, catenary and constant stress vaults. Elastic and viscous compression has been eliminated.

Figure 17 reveals the differences between the vaults. The difference increases as the height of the arch is increased. As the vault height is reduced, the catenary and constant stress vault approaches the parabolic vault.

Bending stresses due to settled shapes in snow vaults

In the case of snow vault structures, the optimum shape can only be achieved temporarily, when the elastic and viscous compression of the snow has been eliminated by artificially increasing the thrust force of the vault. This can be achieved by increasing the compression force at the crown, between the vault halves, by installing hydraulic jacks or by reducing the distance between the vault supports. As the compression increases over time, it may be necessary to increase the thrust again.

The snow vault is sensitive to rapid settlement due to its viscous behaviour. Deformations of snow can be studied computationally as viscous deformations of snow [1]. The viscosity properties of snow are strongly dependent on the density of the snow. It is recommended to use as dense snow as possible for vault structures [2].

Calculation examples of deformed vaults

The effect of the deformed shape on the stresses is illustrated below using two example cases. The calculation has been carried out assuming that the base of the vault is rigid. The self-weight is the weight of the original constant stress vault. The length of the settled

vault is shorter than the original vault, so the original weights given in the calculation represent the compaction of the snow with increased unit weight.

The vaults have settled shapes as shown in Figure 18. The settlements at the crown are $h/8$ equal to 0.625 m, corresponding to the maximum value allowed by the design guidelines RIL 218-2001 [1].

In the calculations, the thickness of the vault at the crown is 1.0 m. The span is 10 m and the height of the vault is 5 m. The unit weight of the snow used is 0.005 MN/m^3 . The constant stress calculated for the original vault is 0.02 MPa.

Simple FEM calculations using the established shapes with beam elements show that the "wrong" shape changes the stresses significantly. The calculated bending moments are shown in Figure 19 and the corresponding stresses in Figure 20.

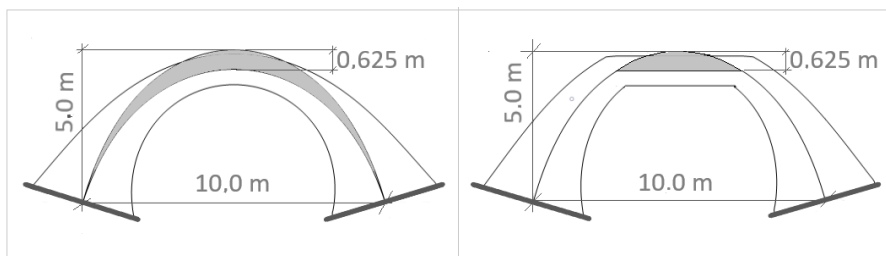


Figure 18. Settled snow vaults.

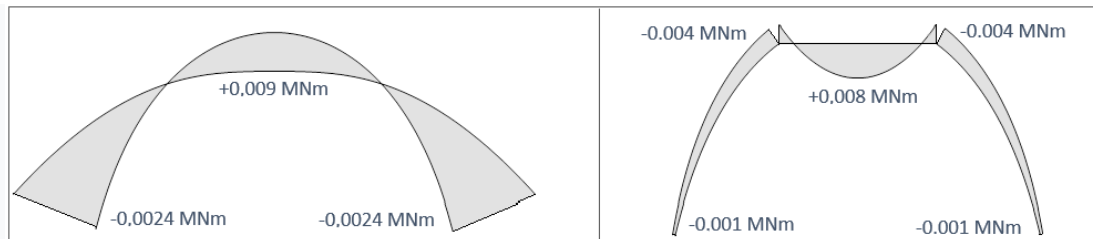


Figure 19. Bending moments of the vaults due to "wrong" shapes.

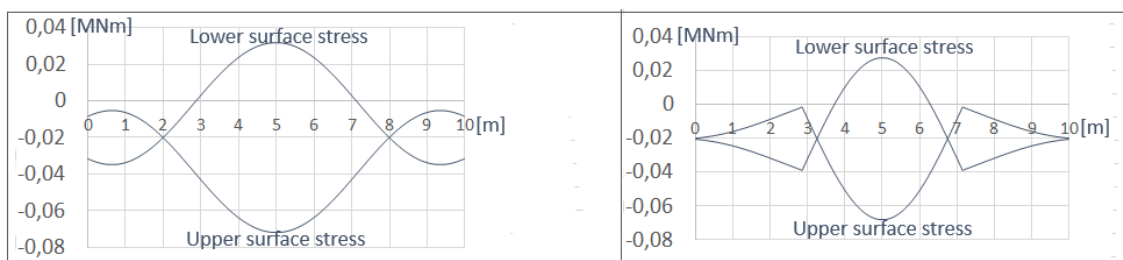


Figure 20. Stresses in the vault of the settled forms.

Shear stresses are generated in the settled vault due to the bending moments caused by the eccentricity of the thrust line. The shear stresses together with the bending stresses can in worst case lead to the collapse of the vault.

Summary

In snow vaults, the dead load is usually the biggest load. The shape of the arch has a decisive influence on its load-bearing capacity. The rapid and large viscous deformations of the snow emphasise the importance of shape analysis, and computational methods are required to calculate the deformations. The settlements should be monitored and the bearing capacity calculated according to the deformed shape.

The size of the snow load on the vault should be monitored and a good aim is to keep the snow thickness in line with the calculations. Locally added snow will not normally improve the bearing capacity of the vault.

The shape of the vault formwork does not match the shape of the central axis of the vault. The vault formwork must be shown on the structural drawings. The thickness of the snow must be shown on the structural drawings. The drawings should indicate the weight of additional snow allowed due to snowfall. Snow removal may be required.

It would seem that the constant stress vault is the most efficient form of snow vault. However, the published instructions for snow structures do not yet recognise the constant stress vault. It may therefore be helpful to supplement the published snow construction design instructions, especially with regard to vault and dome structures. It would also be beneficial to conduct further research and practical testing of snow structures.

Acknowledgements

This research has been supported by the Interreg NPA project NPA0500141 Northern Buildings in Changing Climate. This support is gratefully acknowledged.

References

- [1] RIL 218-2002. Snow constructions – General rules for design and construction ISBN:951-758-421-0.
- [2] Rynnänen, K. Safe Snow and Ice Construction to Arctic Conditions, The Interconnected Arctic–UArctic Congress 2016, pp. 277–282, 2017. https://link.springer.com/chapter/10.1007/978-3-319-57532-2_28
- [3] Gerhardt, R., K.-E., & Pichler, G. The methods of graphical statics and their relation to the structural form. In S. Huerat (Ed.) Proceedings of the First International Congress on Construction History, pp. 997–1006, 2003.
- [4] Tyas, A., Pichugin, A. V., & Gilbert, M. Optimum structure to carry a uniform load between pinned supports: exact analytical solution. *Proceedings of the Royal Society A: Mathematical, Physical and Engineering Sciences*, 467(2128), 1101–1120, 2010. <https://doi.org/10.1098/rspa.2010.0376>
- [5] Hooke, R. Lectures de potentia restitutiva, or of spring explaining the power of springing bodies. London: John Martyn, 1678.
- [6] Bukowski, J. Christiaan Huygens and the problem of the hanging chain. *The College Mathematics Journal*, 39(1), 2–11, 2008. <https://doi.org/10.1080/07468342.2008.11922269>
- [7] Hann, J., Moseley, H., Stevenson, R., Hosking, W., & Hughes, T. *Theory, practice, and architecture of bridges*, pp. 388–389, 1843. London: Architectural

- Laboratory, High Holborn, Berlin: Springer-Verlag.
- [8] Heyman, J. Hooke's cubio – parabolic conoid. *The Royal Society Journal of History of Science: Notes and Records*, 52(1), 39–50, 1998.
<https://doi.org/10.1098/rsnr.1998.0033>
 - [9] H Alassi, S. Jacob Bernoulli and the problem of catenary: Mechanics of Jacob Bernoulli. Paper presented at BSHS Conference, Manchester, UK, 2019.
<https://www.researchgate.net/publication/332028799>
 - [10] Marano, G. C., Trentadue, F., & Petrone, F. Optimal arch shape under static vertical load. *Acta Mechanica*, 225(3), 679–686, 2013.
<https://doi.org/10.1007/s00707-013-0985-0>
 - [11] Marano, G. C., Trentadue, F., Grego, R., Vanzi, I., & Briseghella, B. Volume/thrust optimal shape criteria for arches under static vertical loads. *Journal of Traffic and Transportation Engineering*, 5(6), 503–509, 2018.
<https://doi.org/10.1016/j.jtte.2018.10.005>
 - [12] Lewis, W, J. Constant stress arch and their design space. *Proceedings of the Royal Society A: Mathematical, Physical and Engineering Sciences*, 2022.
<https://doi.org/10.1098/rspa.2021.0428>
 - [13] Järvenpää, E., & Jutila, A. Ultimate spans and optimal rise relations of steel arches. 20 th Congress of IABSE, The Evolving Metropolis, Report, pp. 991–995, 2019. New York City.
 - [14] Lewis, W. Form-finding design. Warwick Research Seminar.
https://warwick.ac.uk/fac/sci/eng/research/research_lunch_seminars/20180427wl_form_finding_design.pdf, 2018.
 - [15] Nikolic, D. Catenary arch of finite thickness as optimal arch shape. *Structural and Multidisciplinary Optimization*, 60(5), 1957–1966, 2019.
<https://doi.org/10.1007/s00158-019-02304-9>
 - [16] Handy R.L., “The Igloo and the Natural Bridge as Ultimate Structures”, Engineering Research Institute and Civil Engineering Dept. Iowa. Arctic, 1973.
 - [17] Williams, C. What is a shell. [Printed lecturing material]. University of Bath, 2016.

Esko Järvenpää, Antti H. Niemi
Civil Engineering Research Unit, Faculty of Technology, University of Oulu, Pentti
Kaiteran katu 1, 90570 Oulu, Finland

Matti-Esko Järvenpää
WSP Finland Oy